

# Micromachined lens microstages for two-dimensional forward optical scanning

Hyeon-Cheol Park, Cheol Song and Ki-Hun Jeong\*

Department of Bio and Brain Engineering, Korea Advanced Institute of Science and Technology (KAIST),  
Daejeon, Korea  
\*kjeong@kaist.ac.kr

**Abstract:** This work presents a novel approach for a miniaturized optical scanning module based on lateral and piston motion of two commercial lenses by MEMS actuation. Two aspheric glass lenses of 1 mm diameter are assembled on two electrostatically actuated microstages moving along perpendicular axes to tilt optical path. The compact integration secures the effective beam aperture of 0.6 mm within the device width of 2 mm. The lens mass provides high-Q motions at low operating voltages of DC 5 V and AC  $10 V_{pp}$ , i.e., the lateral angle of  $\pm 4.6^\circ$  at 277 Hz and the vertical angle of  $\pm 5.3^\circ$  at 204 Hz. The device can provide a new direction for miniaturizing laser scanning based endoscopes or handheld projectors.

©2010 Optical Society of America

**OCIS codes:** (120.3890) Medical optics instrumentation; (120.5800) Scanners; (220.4000) Microstructure fabrication; (230.3990) Micro-structure devices;

---

## References and links

1. W. Piyawattanametha, E. D. Cocker, L. D. Burns, R. P. J. Barretto, J. C. Jung, H. Ra, O. Solgaard, and M. J. Schnitzer, "In vivo brain imaging using a portable 2.9 g two-photon microscope based on a microelectromechanical systems scanning mirror," *Opt. Lett.* **34**(15), 2309–2311 (2009).
2. J. T. C. Liu, M. J. Mandella, H. Ra, L. K. Wong, O. Solgaard, G. S. Kino, W. Piyawattanametha, C. H. Contag, and T. D. Wang, "Miniature near-infrared dual-axes confocal microscope utilizing a two-dimensional microelectromechanical systems scanner," *Opt. Lett.* **32**(3), 256–258 (2007).
3. R. A. Conant, J. T. Nee, K. Y. Lau, and R. S. Muller, "A flat high-frequency scanning micromirror," in *Proceedings of the Solid-State Sensor and Actuator Workshop*, (Transducers Research Foundation, Cleveland, Ohio, 2000), pp. 6–9.
4. H. Toshiyoshi, G. D. J. Su, J. LaCrosse, and M. C. Wu, "A surface micromachined optical scanner array using photoresist lenses fabricated by a thermal reflow process," *J. Lightwave Technol.* **21**(7), 1700–1708 (2003).
5. A. Jain, and H. Xie, "An electrothermal microlens scanner with low-voltage large-vertical-displacement actuation," *IEEE Photon. Technol. Lett.* **17**(9), 1971–1973 (2005).
6. C. P. B. Siu, H. Zeng, and M. Chiao, "Magnetically actuated MEMS microlens scanner for in vivo medical imaging," *Opt. Express* **15**(18), 11154–11166 (2007), <http://www.opticsinfobase.org/VJBO/abstract.cfm?URI=oe-15-18-11154>.
7. S. Kwon, and L. P. Lee, "Micromachined transmissive scanning confocal microscope," *Opt. Lett.* **29**(7), 706–708 (2004).
8. K. Takahashi, H. N. Kwon, M. Mita, K. Saruta, J.-H. Lee, H. Fujita, and H. Toshiyoshi, "A silicon micromachined  $f$ - $\theta$  micro lens scanner array by double-deck device design technique," *IEEE J. Sel. Top. Quantum Electron.* **13**(2), 277–282 (2007).
9. X. Liu, M. J. Cobb, Y. Chen, M. B. Kimmey, and X. Li, "Rapid-scanning forward-imaging miniature endoscope for real-time optical coherence tomography," *Opt. Lett.* **29**(15), 1763–1765 (2004).
10. T. Ota, H. Fukuyama, Y. Ishihara, H. Tanaka, and T. Takamatsu, "In situ fluorescence imaging of organs through compact scanning head for confocal laser microscopy," *J. Biomed. Opt.* **10**(2), 024010 (2005).
11. Y. Wang, M. Bachman, G. P. Li, S. Guo, B. J. F. Wong, and Z. Chen, "Low-voltage polymer-based scanning cantilever for in vivo optical coherence tomography," *Opt. Lett.* **30**(1), 53–55 (2005).
12. Y. Fukuta, H. Fujita, and H. Toshiyoshi, "Vapor Hydrofluoric Acid Sacrificial Release Technique for Micro Electro Mechanical Systems using Labware," *Jpn. J. Appl. Phys.* **42**(Part 1, No. 6A), 3690–3694 (2003).
13. Y. S. S. Chiu, K. D. J. Chang, R. W. Johnstone, and M. Parameswaran, "Fuse-tethers in MEMS," *J. Micromech. Microeng.* **16**(3), 480–486 (2006).
14. S. S. Rao, *Mechanical Vibrations*, (Reading: Addison-Wesley, 1990), Chap. 3.

15. H. J. Shin, M. C. Pierce, D. Lee, H. Ra, O. Solgaard, and R. Richards-Kortum, "Fiber-optic confocal microscope using a MEMS scanner and miniature objective lens," *Opt. Express* **15**(15), 9113–9122 (2007), <http://www.opticsinfobase.org/VJBO/abstract.cfm?URI=oe-15-15-9113>.
- 

## 1. Introduction

Optical scanning plays functional roles in many applications including optical sensing, imaging, and display devices. Recently, the compact packaging becomes of great interest for *in-vivo* endoscopy or microprojection applications. Current state-of-the-art microelectromechanical system (MEMS) techniques contribute to the effective miniaturization of the optical scanning systems based on micro-mirrors [1–3], micro-lenses [4–8] or fibers [9–11]. However, the MEMS mirror or lens based previous works require relatively large space compared to the effective clear aperture size due to the in-plane configuration of all the optical and mechanical components. Besides, they also entail precise alignment between multiple optical components in vertical assembly under an optical microscope. The fiber-based methods, in contrast, provide simple alignment and packaging but high wavelength sensitivity.

This work presents a novel approach for a miniaturized optical scanning module based on lateral and piston motion of two commercial lenses by MEMS actuation. The module includes a fiber collimator and two aspheric glass lenses, which are laterally integrated on the top of each microstage with silicon lens holders. The lens holders help a simple alignment during the integration. During the layout design, the position and size of lens holder structures have been determined after the optical design. Two-dimensional optical scanning can be achieved by the perpendicular motion of two glass lenses. The microstage can be electrostatically actuated by a lateral comb drive for lateral motion or a vertical comb drive for piston motion. The microstage thickness and the lens diameter determine the front dimension along the optical axis. This configuration helps increment of the clear aperture within a given space so that it can provide a capability for higher numerical aperture. Moreover, the lens integration can also offer high mechanical Q-factor at low operating voltage.

## 2. Optical design of the lens microstage

The MEMS two-dimensional lens microstages comprise three parts of collimation, scanning, and focusing. A fiber collimator (LightPath Technologies, Inc., lens diameter: 1.25 mm, beam diameter: 0.6 mm) and two scanning aspheric glass lenses (ALPS Electric Co., LTD., lens diameter: 1 mm,  $f = 0.5$  mm, clear aperture: 0.6 mm) are employed. An objective lens (Edmund Optics, Inc,  $f = 20$  mm, NA = 0.25) is added to focus the beam on image plane. The objective lens is not included on the scanner module to open the appropriate selection of an objective lens depending on imaging modalities, e.g., a low NA objective lens for optical coherence tomography (OCT) or a high NA objective for higher resolution confocal microscopy.

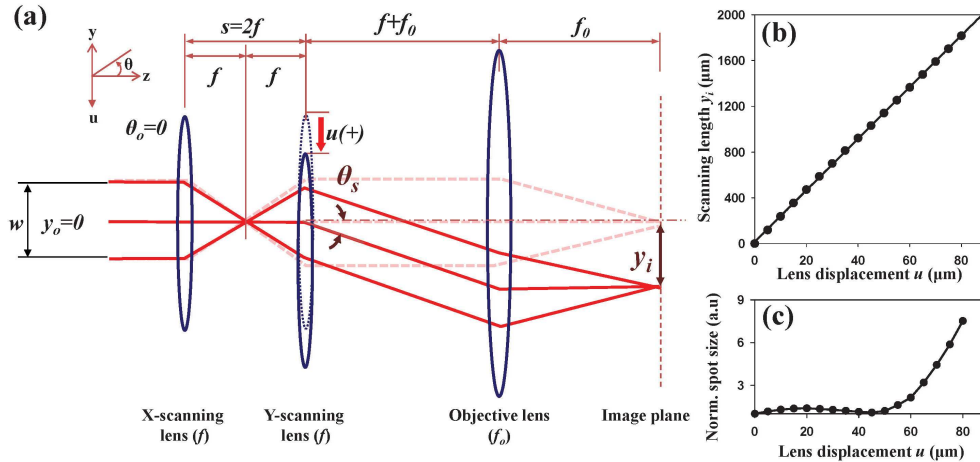


Fig. 1. (a) The optical layout of lens based two-dimensional scanning module consisting of a collimating lens, x and y scanning lenses and an objective lens. (b) Linear relationship between scanning length  $y_i$  and lens displacement  $u$ . (c) The variation of beam spot size along the lens displacement.

Figure 1 shows the optical layout of the lens scanning module as well as the optical simulation results of the scanning characteristics with the optical components described previously. A beam is collimated, focused by an aspheric glass lens for x-scanning in lateral direction and re-collimated by another lens for y-scanning in vertical direction. The beam is finally refocused on the image plane by an objective lens. The distance between two scanning lenses  $s$  is set to be  $2f$  to obtain the re-collimation, where  $f$  is the focal length of the scanning lens. The objective lens is then placed at the sum of focal lengths  $f$  and  $f_o$  behind the second scanning lens. Figure 1(a) shows two-dimensional optical scanning can be implemented by orthogonally moving the first and the second scanning lenses. Then, the scanning angle  $\theta_s$  and the scanning length at the image plane  $y_i$  can be determined by  $-uf$  and  $-(f_o/f)u$ , where  $u$  is the displacement of scanning lens. Figure 1(b) shows that the scanning length is linearly proportional to the lens displacement.

The angular resolution is determined by the Rayleigh criterion of  $1.22\lambda/w$ , where  $w$  is the beam diameter. The number of *resolvable spots* is determined by dividing total scanning angle into the angular resolution. The value is not relevant to the objective lens but both the numerical aperture and the displacement of the scanning lens [15]. Therefore, the maximum resolvable spots can be improved by increasing either numerical aperture of the scanning lens, i.e.,  $w/2f$ , or the lens displacement. The lens displacement is still limited by the off-axis aberrations during the lens motion. However, the optical simulation result shows that the light can be scanned until the lens displacement of  $\pm 50 \mu\text{m}$  without significant degradation of angular resolution as shown in Fig. 1(c). The calculated scanning angle is  $\pm 5.7^\circ$  at the lens displacement of  $\pm 50 \mu\text{m}$  and the scanning resolution is  $0.074^\circ$ . Consequently, the calculated maximum number of resolvable spots is 154 by 154 spots at a wavelength of 633 nm.

### 3. Microfabrication procedure and lens integration

The two-dimensional lens microstages are monolithically fabricated on a heavily boron doped silicon-on-insulator (SOI) wafer by a two-step deep reactive ion etching (DRIE) process. The resistivity of the SOI wafer is between  $0.001 \Omega\text{-cm}$  and  $0.005 \Omega\text{-cm}$ . The detail microfabrication procedures are described in Fig. 2.

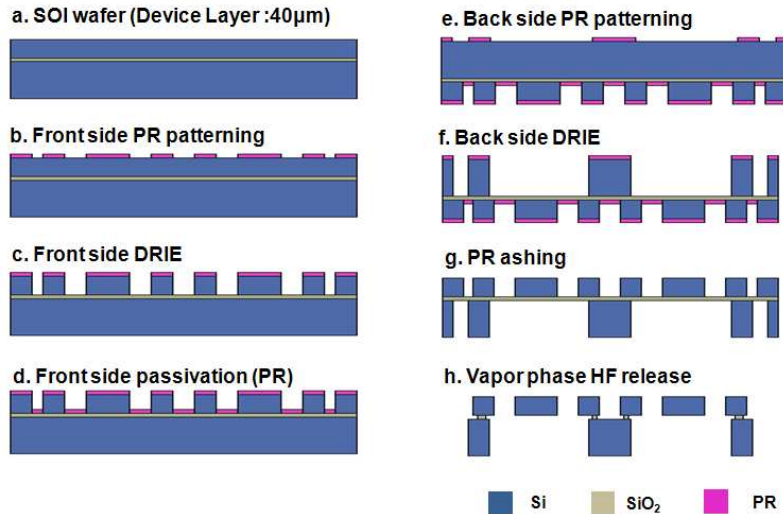


Fig. 2. Microfabrication procedure for 2D MEMS lens scanning modules at wafer level.

First, the microstages with lens holders are defined on the 40  $\mu\text{m}$  thick top silicon layer by DRIE using an etch mask of a negative photoresist (JSR Corp., THB110N) (Figs. 2(b), 2(c)). The 400  $\mu\text{m}$  thick bottom silicon is then etched with masking layers of thick photoresist (JSR Corp., THB126N) to secure the spacing for lens motion (Fig. 2(f)). During the etch of the bottom layer, the microstructure may have some fracture due to the rupture of the buried oxide induced by thermal stress. The problem can be cleared by protecting the top layer with a 5  $\mu\text{m}$  thick negative photoresist as a passivation layer (Fig. 2(d)). After the etching process, the passivation layer is removed with oxygen plasma (Fig. 2(g)). The device is then released by removing the 2  $\mu\text{m}$  thick buried oxide layer with vapor-phased hydrofluoric acid (HF) to avoid the sticking problem of microstructures by the surface tension of the liquids (Fig. 2(h)) [12]. Figure 3(a) shows the SEM picture of the micromachined scanning module.

After the microfabrication process, each chip is separated from the wafer by disconnecting silicon tether structures by Joule heating (pointed in Fig. 3(a)) [13]. Finally, the two-dimensional lens microstages are completed by mounting lenses with an ultraviolet (UV) curable optical adhesive. With a pressurized glass pipette, a UV-curable epoxy monomer is precisely dispensed on the lens holders of the microstages. An aspheric glass lens is carefully mounted on the lens holders by using a vacuum tweezer with micromanipulation. The UV curable epoxy resin is evenly spread out over the gap between the aspheric glass lens and the lens holder due to capillary forces and polymerized by UV exposure. Consequently, the lenses are precisely self-aligned and attached on the lens holders.

The piston motion of the microstage may require the vertical offset between the upper and lower comb fingers for electrostatic actuation. The requirement results in a complicate fabrication process with low yield. However, the resonant scanning may not need the initial offsets. Therefore, all the movable elements of the two-dimensional lens microstages are defined with in-plane configurations using a single mask. The simple procedure provides the yield over 90 percents at the whole wafer level. Figures 3(b) and 3(c) shows the perspective view of the final device. The whole system is built in a dimension of  $2 \times 2.7 \times 5.5 \text{ mm}^3$ . By integrating lenses perpendicularly on MEMS actuators, more compact device size along the optical axis is accomplished within 2 mm, even though the integrated lenses have a diameter of 1 mm.

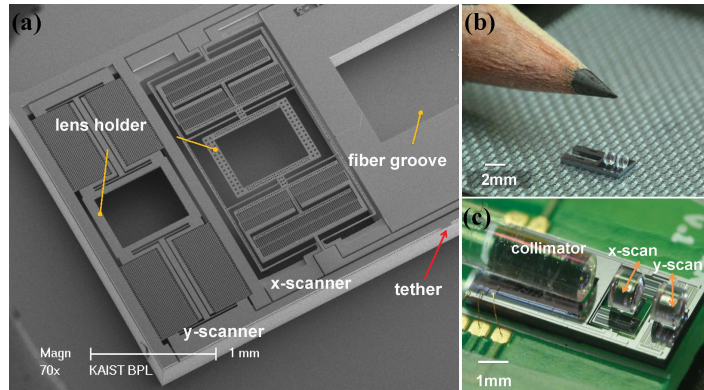


Fig. 3. (a) SEM image of the fabricated device. MEMS actuators, microstructures for integrating optical components, i.e., lens holders and fiber grooves, and tether structures to separate device from the wafer are integrated on a chip satisfying both optical and mechanical requirements. (b), (c) Perspective view of the 2D lens microstage. Fiber collimator and scanning lenses are integrated on a chip within a dimension of  $2 \times 2.7 \times 5.5 \text{ mm}^3$ .

#### 4. Device characterization

The orthogonal lens scanning has been demonstrated by actuating the microstages with electrostatic comb drives. Figure 4 shows the frequency responses of the lens microstages. For the spring-mass-damper system, the resonant frequencies are inversely proportional to the square root of the mass, while the quality factor (Q-factor) has the opposite relationship [14]. Consequently, the lens integration induces the resonance frequency shift and the Q-factor enhancement. The heavy mass of the lens ( $2 \text{ mg}$ ), which is about 70 times heavier than that of the device, shifts the resonant frequencies 87% lower than before the lens integration. The measured resonant frequencies are 277 Hz and 204 Hz for lateral and piston motion, respectively. Besides, the Q-factor is increased from 35 to 277. The high Q value increases the energy confinement at the resonant frequency so that it minimizes the operating voltages at resonance. For example, under DC 5 V and AC 10 V<sub>pp</sub> voltages, the lateral and piston motion show 40 μm and 46 μm in the amplitude, respectively. In turn, they also correspond to the scanning angle of 4.6° and 5.3°. Without lens, however, the lateral motion amplitude is only 15 μm with DC 20V biased operation voltage and no piston motion is observed due to nanoscale static offset between vertical comb fingers. On the other hand, the heavy lens mass may lead to the orientation dependency of the scanners due to gravitational force. All the scanners have been designed to have very high stiffness ratios between the motion direction and the others to conserve the mechanical stability.

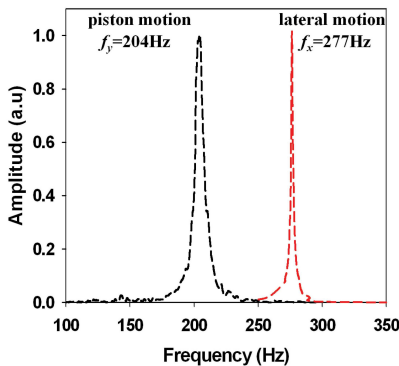


Fig. 4. Frequency response of the lens microstages. The lateral resonance is at 277 Hz and piston resonance is at 204 Hz.

The two-dimensional optical scanning has also been demonstrated. HeNe laser at 633 nm was used for the visualization of beam scanning. The collimating beam was directly coupled through the scanning lenses. Note that the fiber collimator of the scanning module is initially set to single mode at 1310 nm. The scanning beam path was captured using a CCD camera (Canon,  $5.71\ \mu\text{m} \times 5.71\ \mu\text{m}$  pixel size) as shown in Fig. 5(a) -5(d). The focal spot size without scanning is measured to  $17\ \mu\text{m}$ , which corresponds to  $0.087^\circ$  in angular resolution. The lateral and vertical scan lengths are  $891\ \mu\text{m}$  and  $1040\ \mu\text{m}$ , respectively and the measured resolvable spots are 104 by 122 spots.

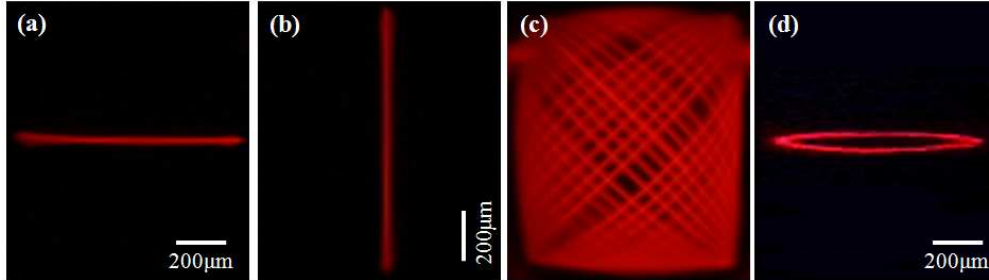


Fig. 5. Two-dimensional optical scanning demonstration; (a) x-scanning, (b) y-scanning, (c) 2D Lissajous pattern.  $891\ \mu\text{m} \times 1040\ \mu\text{m}$  scanning area is achieved under the resonance excitation. (d) Elliptical scanning pattern excited at the same frequency. Since piston motion is not excited at resonance, y-scanning is much smaller than x-scanning.

## 5. Conclusion

The two-dimensional optical scanning has been successfully demonstrated by implementing the orthogonal motion of two commercial glass lenses on the active microstages at low operating voltages. The lens holder effectively provides a simple optical alignment with commercial quality aspherical lenses of millimeters in diameter. Furthermore, the lateral integration of the glass lenses on top of the microstages secures the device compactness along the optical axis. The device is integrated on a single chip with a dimension of  $2 \times 2.7 \times 5.5\ \text{mm}^3$ . The maximum scan angle is  $\pm 4.6^\circ$  in x-scanning and  $\pm 5.3^\circ$  in y-scanning with the angular resolution of  $0.087^\circ$ .

The device is now being optimized for OCT or confocal microscopy based *en-face* endoscopic imaging regarding on aberration correction objectives [15]. The device can provide a new direction for miniaturizing laser scanning based forwarding endoscopic imaging or even microprojection.

## Acknowledgements

The authors would acknowledge Prof. Ming C. Wu at UC Berkeley for helpful discussion and all staff at the NNFC (KAIST National Nanofab Center) for their technical support. This work was supported by the National Research Foundation grant (NRF No. 2010-0000210) and the Industrial Strategic Technology Program of the Ministry of Knowledge Economy (KI001889) grant funded by the Korea Government.